Article:

Aftab, N, Zaidi, SAR and McLernon, D orcid.org/0000-0002-5163-1975 (2020) Scalability analysis of multiple LoRa gateways using stochastic geometry. Internet of Things, 9. 100132. ISSN 2199-1073

https://doi.org/10.1016/j.iot.2019.100132

Scalability Analysis of Multiple LoRa Gateways using Stochastic Geometry

Noman Aftab, Syed Ali Raza Zaidi, Des McLernon

School of Electronic and Electrical Engineering, University of Leeds, UK

Abstract

Low-Power Wide Area Networking (LPWAN) technology offers long-range communication, enabling new types of services for Internet-of-Things (IoT). While LPWAN solutions are proliferating verticals at tremendous pace, little attention has been paid to scalability and performance analysis of such networks. Hence, it is of utmost importance to analyze how well these technologies will scale as the number of connected devices grows in future. Several technologies are associated with LPWANs, but Longe Range WAN (LoRaWAN) is the most adopted LPWAN technology worldwide. It promises ubiquitous connectivity in outdoor IoT applications while keeping network structures and management as simple as possible. Consequently LORAWAN has received a lot of attention in recent time from network providers. In this letter, we first perform the system level outage analysis of a single LoRa gateway by using the chirp spectrum modulation scheme. We then extend our investigation to multiple gateway scenario and show that the coverage probability reduces exponentially when the number of gateways increases due to the presence of more interfering signals from different nodes using the same spreading sequence. We conclude that this fundamental limiting factor is perhaps more significant towards LoRa scalability. Our derivations for co-spreading factor interference found in multiple LoRa gateways enables demand of scalability analysis of such networks.

Keywords: LoRa, IoT, Scalability, Multiple gateways.

1. Introduction

Large deployments of the Internet of Things (IoT) are becoming reality and are enabling new business models for verticals like intelligent transportation systems, environmental monitoring and many more. Large numbers of these IoT deployments are using Low-Power Wide-Area Networks (LP-WAN). Current LPWAN technologies like Long Range (LoRa) [1], Sigfox [2], NB-IoT [3],

Email address: elnaf@leeds.ac.uk, s.a.zaidi@leeds.ac.uk, D.C.McLernon@leeds.ac.uk (Noman Aftab, Syed Ali Raza Zaidi, Des McLernon)

RPMA [4] and weightless standard [5] are used for communication over long distances. The LPWANs generally consist of single-hop networks, where each node is connected with at least one sink node (gateway) through RF links making a star topology. Network providers consider this to be advantageous, as building and keeping up a multi-hop system proves to be more complex and expensive. Nonetheless, as LPWANs cover a large range and all the nodes are connected with single or very few gateways so the communication medium is shared by a large number of nodes. The basic question which arises in LPWAN technologies; is "how many numbers of nodes can be successfully implemented in a region without deteriorating the performance of application"? To answer the above-mentioned question, "LoRa", a prominent LPWAN technology is chosen for coverage analysis. The primary reason behind choosing LoRa over the other LPWAN technologies is that it is the most generally deployed LPWAN technology these days and is considered by many industries as a core technology for their future IoT deployments. In this paper, a complete study of LoRa scalability is performed by considering different channel parameters and using different tools form Stochastic Geometry. First of all, a LoRa system-level model is established, in which chirp spectrum modulation (CSS) modulation is implemented and impact on the interference of packets during transmission is investigated. A scalability analysis of a single LoRa gateway is presented and also analysis of how its coverage probability is affected by increasing the node density. This probability is further dependent on two connection probabilities; one is related to SNR, and the other one is related to co-spreading factor interference both are dependent on each other. Later on, the impact of adding more gateways on our coverage probability is studied and it is concluded that adding more gateways in our proposed model will further decrease the coverage probability, hence a novel approach for finding the conditional outage probability for multiple LoRa Gateways is established.

2. Previous Work

Some recent studies [6, 7] have investigated whether LPWAN technologies will support a large number of end devices that are expected to be deployed in future deployments. Only a few studies related to LoRaWAN have been investigated so far. Authors in [8] estimate that the limit on the number of nodes that can be compatible with a typical LoRaWAN deployment is 120 by 3.8 ha, a device density much lower than expected in urban environments. Georgiou et al. in [9] look on the scalability analysis of a single LoRa gateway. They introduce two outage conditions, the first one is related to SINR and the other one is due to the transmission from the same Spreading Factors (SFs) signals and assume that both of these probabilities are independent of each other and hence take their joint distribution after taking their product. They also reveal that the coverage probability of LoRaWAN decreases exponentially with the number of end devices due to increased interference from these end devices. Both of these studies suggest that end devices should adopt the LoRa communication parameters by making use of more powerful base stations and by exploiting the diversity of base stations to overcome this problem. Other research has been performed to address the problem of the capacity of LP-WAN technologies. Mikhaylov et al. in [7] worked on the Scalability analysis of LoRa and concluded that under low traffic, LoRa works fine with fine reliability and coverage with unavoidable substantial delays, low reliability and possibly average performance in terms of downlink traffic. In the authors investigated the effect of using directional antennas or adding multiple gateways for mitigating inter-network interference in LoRa networks. Authors in [10] evaluated the single cell LoRaWAN network scalability in terms of the number of end nodes that can be served using a simulation model based on real measurements. From there results they concluded that LoRa outperforms ALOHA in term of scalability due to its robust Physical Layer.

3. Contributions

Our main focus is on the scalability analysis of a LoRa network in presence of other LoRa gateways and we will analyze the effect on scalability when different nodes of different Gateways controlled by different NetServers start transmitting at the same time causing a new type of interference called inter-network co-spreading factor interference. Although [9] worked on the scalability analysis of a single Lora Gateway but their study does not show any effect of multiple gateways. In this paper, we address these shortcomings of current scalability analysis of LoRa using stochastic geometry. First we design a system level model of LoRa and observe the modulation and demodulation of LoRa packet using CSS modulation. The results from a spectrogram plot show that when there is some interference from another node with same spreading factor (SF), the receiver is unable to decode the packet correctly.

3.1. System Level Performance of LoRa Gateway

LoRa physical layer uses a different scheme for transmitting messages by employing CSS Modulation. To start with, each LoRa chirp can be coded up to SF=12 bits [1]. A specific frequency trajectory is chosen for each of 2^{SF} symbols. This is achieved by shifting the frequency ramp based on the symbol value and thus, each coded chirp is the cyclic shifted version of the reference chirp. Therefore, for every instantaneous frequency trajectory, a sharp edge is observed corresponding to the value of the symbol. Thus the new expression for instantaneous frequency of the coded chirp is

$$f_{lc}(t) = \{ \ f_c + u.\frac{B}{T}.\left(t - \frac{k}{B}\right) + B, \tag{1}$$

where f_c is the central carrier frequency. If $\mu = 1$ an up-chirp is obtained, while $\mu = -1$ corresponds to a downchirp. It is important to mention that for CSS modulation, B corresponds to the spectral occupancy, as well as the difference between the maximum and minimum instantaneous frequency during the chirp and k represents the number of shifted chips. LoRa Radio Layer

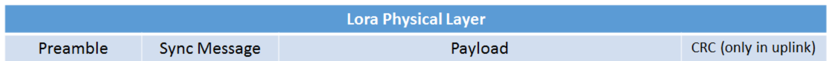

Figure 1: LoRa Radio Layer Format

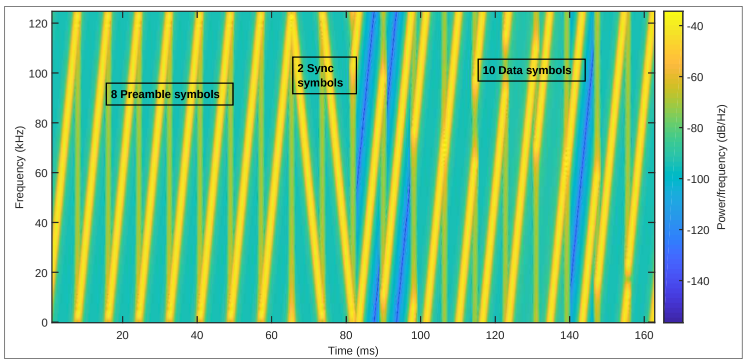

Figure 2: LoRa modulated signal for SF10

modulated message format mainly includes Preamble, Sync, Payload and CRC (only in Uplink) symbols as shown in Fig. 1.

Fig.2 shows the spectrogram of the LoRa Modulated signal for SF $= 10$.

In order to decode the data from the received signal which is cyclic frequency shifted it is multiplied with the inverse chirp (a downchirp for the above case), and so a constant frequency signal is obtained during the symbol part as shown in a) and b) of Fig.3.

When there is some interference due to a packet which is transmitted simultaneously from another node with the same SF and the same frequency, the receiver will unable to properly decode the message in the Data symbol part which is marked in red as an error as shown in c) and d) of Fig.3.

In this analysis, we deploy a LoRa network with a single uplink gateway which is responsive to all the interference from colliding signals. Stochastic Geometry [11] is used as a special tool for modeling the spatial distribution of devices. By summing over all the interfering transmissions in the network, we can find the stochastic average of the interference power with the help of stochastic geometry. Hence, the shot noise process is usually modeled as an interference where Poisson distributed time instants. For the case of random spatial process, the spatial locations of the nodes replace the time instants, whereas the path loss model replaces the impulse responses related to those time instants. In this model the gateway is located at the origin and end devices are randomly deployed uniformly in a region $\mathcal{V} \subseteq \mathrm{R}^2$ as shown in Fig. 4, which is a homogeneous Poisson Point Process (PPP) having intensity function $\lambda > 0$ in $\mathcal{V}$ and 0 otherwise. Each device in a represented by each point in the Poisson Process. For analysis we take $\mathcal{V}$ as a disc having radius $R = 12$ Km and area

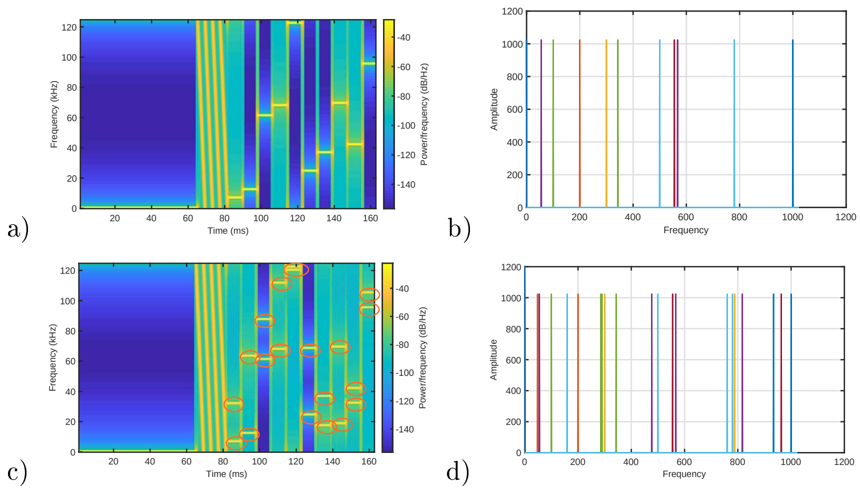

Figure 3: a) LoRa decoded message after inverse chirp multiplication b) DFT of Received LoRa Signal c) LoRa decoded message after inverse chirp multiplication in the presence of interference d) DFT of the Received LoRa Signal in the presence of interference.

$\mathcal{V} = |V| = \pi R^2$ containing total N number of devices and d_i represents the distance between specific end device i and the gateway which is placed at the origin.

Following , the outage probability actually dependent upon the two connection probabilities are defined for a desired signal in uplink mode at the gateway, which are

1. H_1 is the connection probability when SNR of the received signal is greater than the certain threshold q_{SF}, where q_{SF} is directly associated with SF as given in Tab.1
2. Q_1 is the connection probability if any other cocurrent transmission with same SF is also happening, then the desired received signal is at-least 6 dB more stronger than particular cocurrent transmission.

After combining the two connection probabilities, we get the joint outage probability J_1 of the received signal, that can be given by the complement of successfully received signal

$$J_1 = 1 - H_1 Q_1 \tag{2}$$

3.1.1. Outage probability treating the connection probabilities are independent

In the first scenario analyze situation where $H_1$and Q_1 are treated as independent events as in literature where H_1 is given as

$$H_1 = P\left[SNR \geq q_{\text{SF}} \mid d_1\right], \tag{3}$$

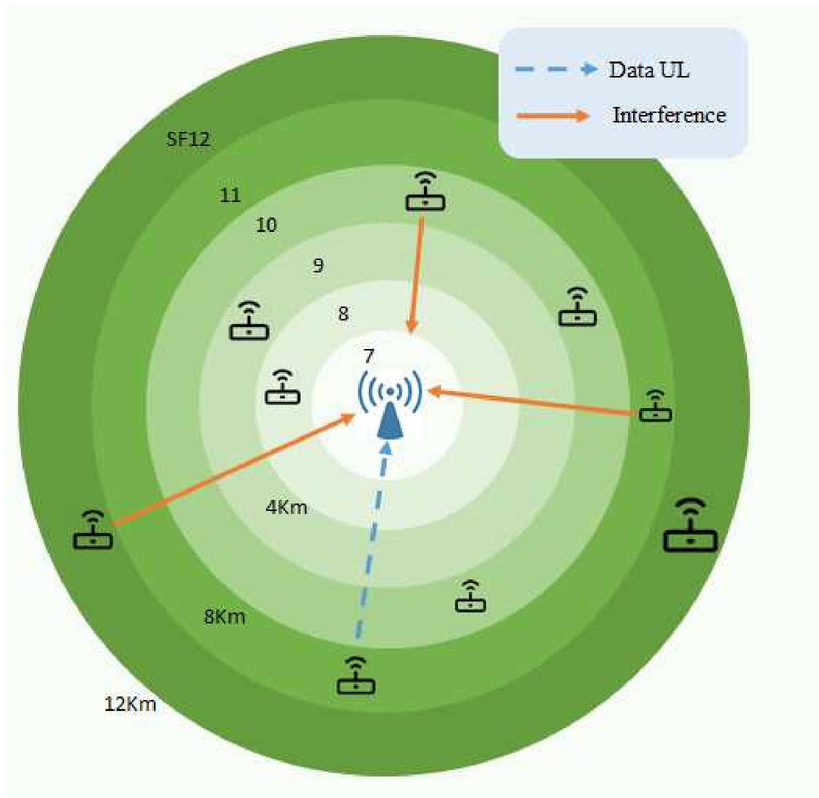

Figure 4: LoRa system model of a single gateway and multiple end devices (can transmit concurrently), located uniformly in a region of radius R km randomly deployed uniformly in a region $\mathcal{V} \subseteq \mathrm{R}^2$

where H_1 is the connection probability which depends on SNR, In Eq. (3) q_{SF} is the threshold SNR (in dBm) for each SF given by Table 1and is defined as the minimum ratio of wanted signal power to noise that can be demodulated. The performance of the LoRa modulation itself, forward error correction (FEC) techniques and the spread spectrum processing gain combine to allow significant SNR improvements. The lower this number the more sensitive the receiver will be. Negative numbers indicate the ability to receive signal powers below the receiver noise floor $\mathcal{N}$ [1] which is the variance of Additive White Gaussian Noise (AWGN) in dBm and it is given by

$$\mathcal{N} = -174 + NF + 10\log_{10}(\mathrm{BW}), \tag{4}$$

in Eq.(4) NF is the receiver noise figure which is fixed at 6 dB and BW is the bandwidth of the receiver.

Moreover LoRa receiver sensitivity S depends upon q_{SF} and $\mathcal{N}$ as

Table 1: LoRa characteristics for a 25 byte message at a bandwidth of 125kHz

SF	SNR q_{SF} dBm	Range Km
7	-6	$l_0 - l_1$
8	-9	$l_1 - l_2$
9	-12	$l_2 - l_3$
10	-15	$l_3 - l_4$
11	-17.5	$l_4 - l_5$
12	-20	$l_5 - l_6$

$$S = \mathcal{N} + q_{\mathrm{SF}} \tag{5}$$

LoRa link budget is given by

$$\text{linkbudget} = P_{\mathrm{i}} - (S) \tag{6}$$

where P_i is defined as the transmitted power of specific end-device i (in milliwatts). The LoRa is capable of changing the spreading factor by doing the trade-off between the network data rate and range requirement and hence $q_{\mathrm{SF}}$and other aforementioned quantities varies accordingly.

The SNR in Eq. (3) is given by

$$\mathrm{SNR} = \frac{P_1 |h_1|^2 g(d_1)}{\mathcal{N}}, \tag{7}$$

where $|h_i|^2$ is the channel gain which is an exponential random variable with mean one. Thus, the outage probability is given by the complement of our connection probability H_1. Eq (3) can be directly calculated by rearranging the SNR, where $|h_1|^2 = \exp{(1)}$, to have

$$H_1 = P\left[|h_1|^2 \geq \frac{\mathcal{N} q_{\mathrm{SF}}}{\mathcal{P}_1 g\left(d_1\right)} \mid d_1 \right] = \exp\left(-\frac{\mathcal{N} q_{\mathrm{SF}}}{\mathcal{P}_1 g\left(d_1\right)} \right). \tag{8}$$

In Eq.(8), $g(d_i)$ is defined as the path loss attenuation function and is given by

$$g(d_i) = \left(\frac{\lambda}{4\pi d_i} \right)^n \tag{9}$$

Friis transmission equation is used for derivation of Eq.(9) having as the wavelength of the carrier signal, whereas $n \geq 2$ is defined as the path loss exponent, normally lies between (2:7)4 in different (sub-) urban environments. As discussed earlier, the second outage condition arises when a signal of same spreading factor (SF) and same frequency from one or more than one end devices start transmitting at the same time, thus causing interference to the original signal. Hence the strongest interfering signal is labeled as k^* given as

$$k^* = arg\, max \left\{ \mathrm{P}_k \chi_k^{SF} \left| h_k \right|^2 g\left(d_k\right) \right\}, \qquad k > 1 \tag{10}$$

since the system under consideration is assumed to be ergodic, (i.e., a system which will not change its statistical properties with time), so time dependency of the received signals can be dropped. In Eq. (10) $\mathcal{X}_k^{SF}$ is the indicator function, which is used to indicate whether a different end device of same frequency and SF is transmitting at the same time with subscript $k > 1$, hence causing interference. It is also assume that the end devices of the same SFs are transmitting with equal power and hence the second outage condition can be found by the complement of second connection probability which is

$$Q_1 = P\left[\frac{{h_1}^2 g(d_1)}{|h_{k^*}|^2 g(d_{k^*})} > 4 \middle| d_1 \right]. \tag{11}$$

For the analysis of co-spreading interference, Eq.(10) and Eq.(11) are used. In order to get second outage condition through Eq. (11), the theory of order statistics (maximum from different independent identically distributed random variables is utilized. We mentioned earlier that the end devices which are located inside the region (described by inner and outer radi i.e., l_j and l_{j+1}km respectively, have the same SF as that of the end device located at $d_1 \in (l_j, l_{j+1})$. This region is denoted by $\hat{\mathcal{V}}(d_1) \subset \mathcal{V}$ which is given as

$$\hat{\mathcal{V}}\left(d_1\right) = \pi\left(l_{j+1}^2 - l_j^2\right), \tag{12}$$

from Eq.(11) $\mathrm{P}\left[\left|h_1\right|^2 g(d_1) > 4\left|h_{k^*}\right|^2 g(d_{k^*})\right]$. As $g\left(d_k\right) = \left(\lambda/4\pi d_k\right)^n$ and introducing a constant c where $c = \left(\lambda/4\pi\right)^n$ and variable $z = \left|h_1\right|^2 g\left(d_1\right)/4$ in Eq. (3.1.1), thus it becomes

$$P\left[\left|h_{k^*}\right|^2 < \frac{\mathrm{z}}{\mathrm{c}}\, d_k^n\right], \tag{13}$$

and its CDF is given by $\mathrm{F}_{X_i(z)} = \int_{l_j}^{l_{j+1}} \left[1 - e^{\left(-\frac{z}{c} d_k^n\right)}\right] . \frac{2\pi d_k}{\left|\hat{V}(d_1)\right|} \mathrm{d} d_k,$
$= 1 - \int_{l_j}^{l_{j+1}} e^{\left(-\frac{z}{c} d_k^n\right)} . \frac{2\pi d_k}{\left|\hat{V}(d_1)\right|} \mathrm{d} d_k$, solving Eq. (3.1.1) we get

$$F_{X_i}(z) = 1 + \beta\left[\frac{2}{n}, \frac{z}{c} l_{l_{j+1}}^n\right] - \beta\left[\frac{2}{n}, \frac{z}{c} l_j^n\right], \tag{14}$$

where is incomplete Gamma function and β is defined as

$$\beta = \frac{2 z^{-\frac{2}{n}} c^{\frac{2}{n}}}{n\left(l_{j+1}^2 - l_j^2\right)}. \tag{15}$$

Now by theory of order statistics we can find the distribution of the strongest interfering signal, X_{k^*}, which is given by

$$F_{X_{k^*}}(z) = E_n\left[\left[F_{X_i}\left(z\right)\right]^n\right], \tag{16}$$

where the sample size n is the random variable, and it is Poisson distributed with mean $v = p_0\rho\,|V(d_1)|$ can be found by expected number of end devices transmitting co currently in the same SF region, $\mathcal{V}(d_1)$ as that of the desired signal. By using the above definitions $F_{X_{k^*}}(x)$ can be written as

$$F_{X_{k^*}}(x) = \sum_{k=0}^{\infty}\left[\left[F_{X_i}(x)\right]^k \frac{v^k e^{-v}}{k!}\right]. \tag{17}$$

By solving Eq. (17) for a Poisson process we have

$$F_{X_{k^*}}(x) = e^{-\left(1-F_{X_i}(x)\right)v}, \tag{18}$$

now by deconditioning on the channel gain we get

$$Q_1 = E_{|h_1|^2}\left[F_{X_{k^*}}\left(\frac{\left|h_1\right|^2 g(d_1)}{4}\right)\right] \tag{19}$$

$$Q_1 = \int_0^{\infty} e^{-z} F_{X_{k^*}}\left(\frac{z\,g(d_1)}{4}\right)\mathrm{d}z. \tag{20}$$

3.1.2. Outage probability when both the connection probabilities are treated jointly

In the previous analysis, we assume that both the outage conditions H_1 and Q_1 are independent from each other and hence take their joint distribution after taking their product, but in reality as Q_1 is also dependent on H_1which in turn depends on SNR, so we defined Q_1 as

$$Q_1(d_1) = E_{|h_1|^2}\left[P\left[\frac{|h_1|^2\,g\,(d_1)}{|h_{k^*}|^2\,g\,(d_{k^*})} > 4 \mid |h_1|^2, d_1\right]\right]. \tag{21}$$

By using Eqs. (11), (19) and (21) we plot the connection probabilities against the distance as shown in Fig.5

Eq.(21) will give us the outage probability. Thus in this case

$$J_1 = 1 - Q_1 \tag{22}$$

Fig. 6 show the monte-carlo simulated results for both the conditional and unconditional outage probabilities J_1.

3.2. Coverage Probability of Multiple LoRa Gateway

In this analysis, we deploy multiple uplink gateways LoRa model as shown in Fig.7 which is sensitive to all the interference from the colliding signals. Stochastic Geometry [11] is used as a special tool for the spatial distribution of devices. In this model the interseted gateway is located at the origin of the disc and end devices are randomly deployed uniformly in a region $\mathcal{V} \subseteq R^2$ as shown in Fig.4 as a homogeneous Poisson Point Process (PPP) having intensity

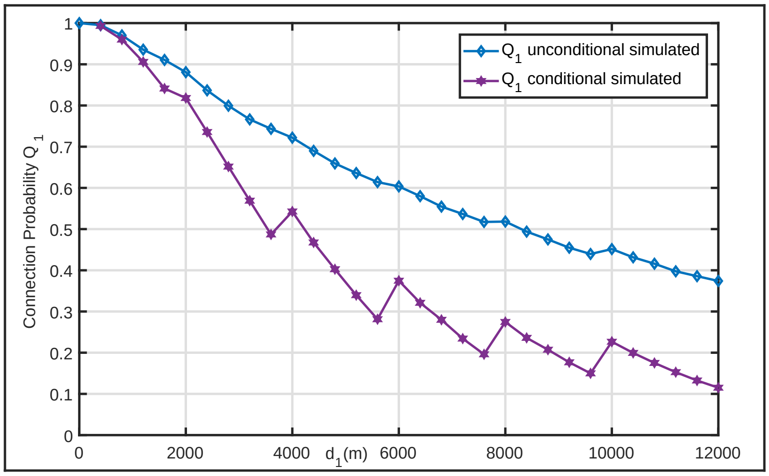

Figure 5: Monte Carlo simulations for connection probability Q_1 (conditional and unconditional)

function $\lambda > 0$ in $\mathcal{V}$ and 0 otherwise. Four other gateways are also present in the vicinity of the main gateway with their nodes, which are also poisoned distributed in a radius of R = 12 Km.

The probability that at any instant of time if a randomly selected device lies in a coverage range (i.e., not in outage) or not is defined as a coverage probability. In order to acquire the coverage probability $\wp_c$ of the system with respect to a variable X, where $X = H_1, Q_1, H_1Q_1$, the deconditioning on the location of the particular end-device by taking average over $\mathcal{V}$ is performed, thus we have

$$\wp_c\left[\chi\right] = \frac{2}{R^2}\int_0^R \chi\left(d_1\right) d_1 \,\mathrm{d}d_1, \tag{23}$$

Now putting $\chi = H_1$ in 23, we get coverage probability for H_1

$$\wp_c[H_1] = \frac{2}{R^2}\int_0^R H_1(d_1) d_1 \,\mathrm{d}d_1, \tag{24}$$

which is a constant quantity due to the fact that $\wp_c[H_1]$ is not dependent on deployment density i.e., $\rho = \bar{N}/\mathcal{V}$. For $\chi = \{H_1, Q_1, H_1Q_1\}$, plot of $\wp_c\left[Q_1\right]$ is shown in Fig.8.

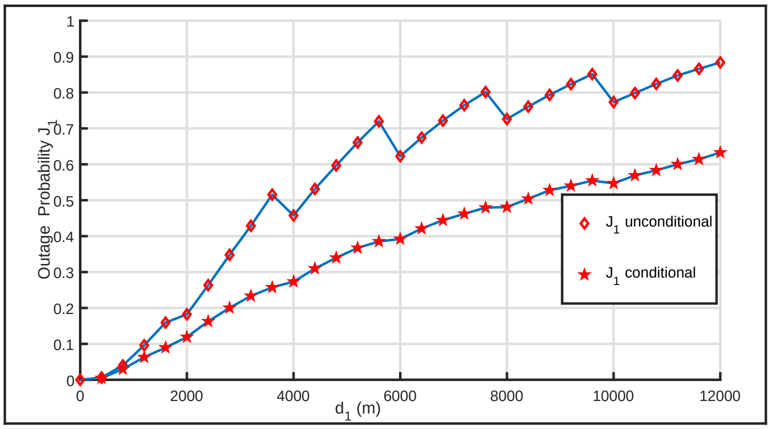

Figure 6: Conditional and unconditional simulation Results for outage probability J_1

4. Numerical Simulations and Discussion

Fig. 2 shows the LoRa modulated signal including preamble, synchronization and data symbols where we can see the transition in frequency/phase in payload (data) symbols. Fig. 3 shows the LoRa decoded message without any interference at the receiver side whereas Fig. 3(a) shows that the receiver is unable to decode the message properly when there is interference from the same SF signal. Fig. 5c) shows Monte Carlo computer simulation results for unconditional connection probability Q_1 as well as Monte Carlo simulated results for conditional connection probability Q_1. For the sake of simplicity, we use Semtech's recommended values of $l_i = 2i \quad \text{for} \qquad i = 0, ...5$ [1]. Each marker In Fig. 5 corresponds to the simulated performance of the single gateway LoRa network in the uplink mode which is averaged over10^5 random deployment realizations of the PPP in $\mathcal{V}$. An Excellent agreement is observed between the derived and simulated results. As threshold q_{SF} is directly related to distance (mentioned in 1st column of Tab.1). In Fig. 6 simulated results of conditional and unconditional outage probabilities are drawn against the distance and further deterioration is observed when both the connection probabilities H_1 and Q_1 are treated jointly(conditional outage probability). For the coverage probability, we use Eq.(23) to plot $\wp_c[Q_1]$ for different number of nodes (end devices) as shown in Fig.8 against the number of gateways. For the coverage probability, we only use $\wp_c[Q_1]$, because that the first coverage probability $\wp_c[H_1]$ remains constant w.r.t. number of nodes (as it only depends on the SNR). It is further observed that by introducing more gateways in the same region will further increase the co-spreading interference as more and more end devices with same SF try to send data simultaneously consequently become the limiting factor for LoRa scalability.

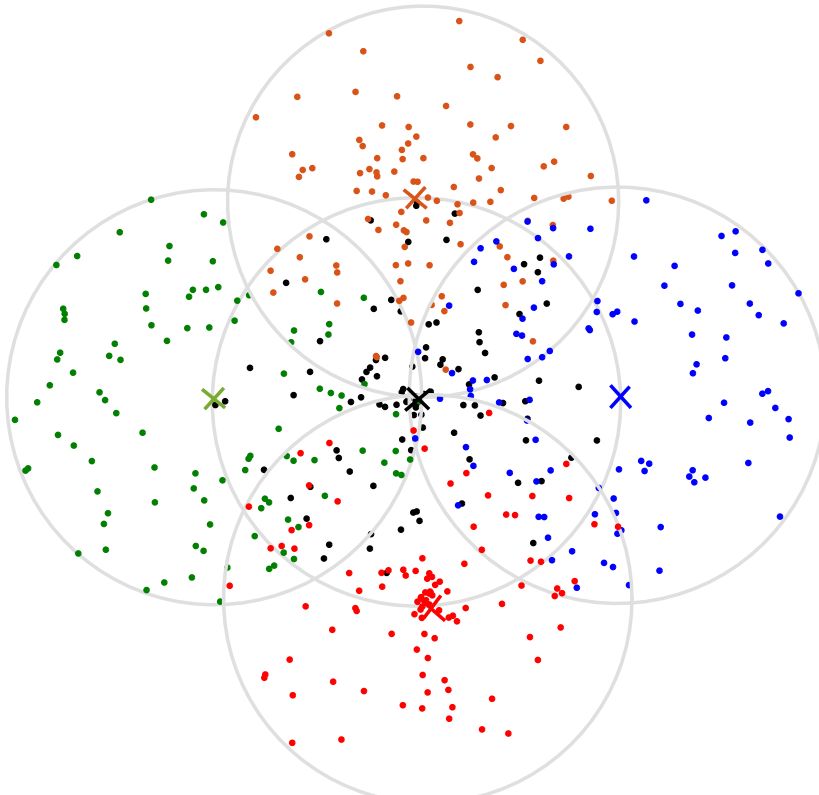

Figure 7: Observed gateway along with four interfering gateways, where each gateway is connected with 100 nodes, all of these nodes are poisoned distributed in a radius $\mathcal{R}$ of 12 Km from their respective gateway. The observed gateway along with its nodes are marked in black whereas other gateways along with their nodes are marked in different colors.

5. Conclusions

In this work, the effectiveness of a LoRa gateway in the presence of other LoRa gateways is investigated. The primary advantage of Lora over other LP-WANs is that it uses a unique modulation scheme called Adaptive CSS, that will extend the communication range if there is no interference present at the channel, but interference can occur when some nodes transmit signals at the same time, frequency and Spreading factor. Moreover, the presence of other LoRa gateways further enhances the interference. The two link connection probabilities are investigated from different tools mentioned in Stochastic geometry. The first link-connection probability is based on SNR and the second one is related to the co-spreading sequence interference. In the first scenario, an Unconditional Outage probability is formed by taking the complement of the product of the above connection probabilities (treated them as independent events). In the second scenario, a conditional outage probability is formed by processing both

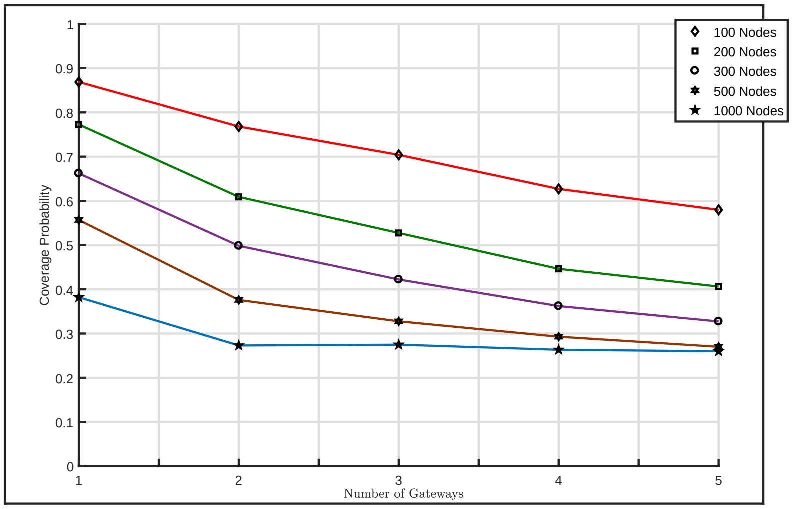

Figure 8: Coverage Probability reduces when more LoRa Gateways introduced for different settings of Number of Nodes

the connection probabilities jointly and taking the complement of the second connection probability only. Both of the conditional and unconditional outage probabilities are plotted against the distance (from the gateway at the origin) and it is concluded that the conditional outage probability degrades rapidly as compare to unconditional outage probability. The coverage probability which changes only due to the second connection probability is also plotted against the number of end devices. By investigating the behaviour of results obtained, which are unique with LoRa, it is found that the second outage probability (due to co-spreading factor) affects both the outage and coverage probability more seriously, despite the fact, there are a lot of mitigation previsions provided in LoRa. It is also concluded that the presence of more LoRa gateways in the same geographical region further deteriorates the performance of the LoRa gateway.

References

[1] Lorawan specification, available:https://lora-alliance.org/, (Accessed 18 September 2017).

[2] Sigfox technology overview, available: https://www.sigfox.com/, (Accessed 07 January 2018).

[3] NB-IoT: Enabling New Opportunities, available: https://gsacom.com/paper/nb-iot-enabling-new-opportunities/, (Accessed 18 April 2018).

[4] RPMA Technology for the Internet of Things, available: https://www.ingenu.com/technology/rpma/, (Accessed 19 March 2018).

[5] Weightless specifications, available: http://www.weightless.org/, (Accessed 21 March 2018).

[6] U. Raza, P. Kulkarni, M. Sooriyabandara, Low power wide area networks: A survey, arXiv preprint arXiv:1606.07360 .

[7] K. Mikhaylov, J. Petaejaejaervi, T. Haenninen, Analysis of capacity and scalability of the LoRa low power wide area network technology, in: European Wireless 2016; 22th European Wireless Conference; Proceedings of, VDE, 1–6, 2016.

[8] M. Bor, U. Roedig, T. Voigt, J. Alonso, Do LoRa low-power wide-area networks scale?, in: The 19th ACM International Conference on Modeling, Analysis and Simulation of Wireless and Mobile Systems, 2016.

[9] O. Georgiou, U. Raza, Low Power Wide Area Network Analysis: Can LoRa Scale?, IEEE Wireless Communications Letters 6 (2) (2017) 162–165.

[10] T. Voigt, M. Bor, U. Roedig, J. Alonso, Mitigating inter-network interference in LoRa networks, arXiv preprint arXiv:1611.00688 .

[11] M. Haenggi, Stochastic geometry for wireless networks, Cambridge University Press, 2012.